

source localizer (0.85 cm versus 1.15 cm) at slightly greater computational expense (1.0 ms versus 0.3 ms) than a comparably tuned system using a Cartesian representation. The hybrid MLP-start-LM method using the new MLP showed the same accuracy as previous systems (0.28 cm) but computation time was reduced from 36 ms to 30 ms. Furthermore, the Soft-MLP was successfully applied to actual MEG data.

A Cartesian output representation cannot encode the location of more than a single dipole. Our use of a distributed output representation was in part motivated by the hope that its greater representational capabilities might allow Soft-MLP networks to be used for multiple dipole localization. The improvements in accuracy for a single dipole were an unexpected benefit, but we will continue our efforts to apply the Soft-MLP architecture to the multiple dipole case.

REFERENCES

- [1] D. E. Rumelhart, G. E. Hinton, and R. J. Williams, "Learning representations by back-propagating errors," *Nature*, vol. 323, pp. 533–536, 1986.
- [2] U. R. Abeyaratne, Y. Kinouchi, H. Oki, J. Okada, F. Shichijo, and K. Matsumoto, "Artificial neural networks for source localization in the human brain," *Brain Topogr.*, vol. 4, pp. 3–21, 1991.
- [3] S. C. Jun, B. A. Pearlmutter, and G. Nolte, "Fast accurate MEG source localization using a multilayer perceptron trained with real brain noise," *Phys. Med. Biol.*, vol. 47, no. 14, pp. 2547–2560, 2002.
- [4] G. E. Hinton, J. L. McClelland, and D. E. Rumelhart, "Distributed representations," in *Parallel Distributed Processing: Explorations In The Microstructure of Cognition, Volume 1: Foundations*, D. E. Rumelhart and J. L. McClelland, Eds. Cambridge, MA: MIT Press, 1986.
- [5] M. Hämäläinen, R. Hari, R. J. Ilmoniemi, J. Knuutila, and O. V. Lounasmaa, "Magnetoencephalography—theory, instrumentation, and applications to noninvasive studies of the working human brain," *Rev. Modern Phys.*, vol. 65, pp. 413–497, 1993.
- [6] R. Caruana, "Multitask learning," *Machine Learning*, vol. 28, no. 1, pp. 41–75, 1997.
- [7] A. I. Ahonen, M. S. Hämäläinen, J. E. T. Knuutila, M. J. Kajola, P. P. Laine, O. V. Lounasmaa, L. T. Parkkonen, J. T. Simola, and C. D. Tesche, "122-channel SQUID instrument for investigating the magnetic signals from the human brain," *Physica Scripta*, vol. T49, pp. 198–205, 1993.
- [8] Y. LeCun, I. Kanter, and S. A. Solla, "Second order properties of error surfaces: learning time and generalization," in *Advances in Neural Information Processing Systems 3*. San Mateo, CA: Morgan Kaufmann, 1991, pp. 918–924.
- [9] A. C. Tang, B. A. Pearlmutter, N. A. Malaszenko, D. B. Phung, and B. C. Reeb, "Independent components of magnetoencephalography: localization," *Neural Computation*, vol. 14, no. 8, pp. 1827–1858, 2002.
- [10] A. C. Tang, B. A. Pearlmutter, M. Zibulevsky, T. A. Hely, and M. P. Weisend, "An MEG study of response latency and variability in the human visual system during a visual-motor integration task," in *Advances in Neural Information Processing Systems 12*. Cambridge, MA: MIT Press, 2000, pp. 185–191.
- [11] J. C. de Munck, A. de Jongh, and B. W. van Dijk, "The localization of spontaneous brain activity: An efficient way to analyze large data sets," *IEEE Trans. Biomed. Eng.*, vol. 48, pp. 1221–1228, 2001.
- [12] R. Van Uitert, D. Weinstein, C. Johnson, and L. Zhukov, "Finite element EEG and MEG simulations for realistic head models: quadratic vs. linear approximations," *J. Biomedizinische Technik*, vol. 46, pp. 32–34, 2001.
- [13] R. H. Kraus Jr., P. L. Volegov, K. Maharajh, M. A. Espy, A. N. Matlashov, and E. R. Flynn, "Performance of a novel SQUID-based superconducting imaging-surface magnetoencephalography system," *Physica C*, vol. 368, no. 1–4, pp. 18–23, 2002.

Independence of Myoelectric Control Signals Examined Using a Surface EMG Model

Madeleine M. Lowery*, Nikolay S. Stoykov, and Todd A. Kuiken

Abstract—The detection volume of the surface electromyographic (EMG) signal was explored using a finite-element model, to examine the feasibility of obtaining independent myoelectric control signals from regions of reinnervated muscle. The selectivity of the surface EMG signal was observed to decrease with increasing subcutaneous fat thickness. The results confirm that reducing the interelectrode distance or using double-differential electrodes can increase surface EMG selectivity in an inhomogeneous volume conductor. More focal control signals can be obtained, at the expense of increased variability, by using the mean square value, rather than the root mean square or average rectified value.

Index Terms—Detection volume, finite-element model, myoelectric control, surface EMG.

I. INTRODUCTION

One of the greatest limiting factors in the development of myoelectric prostheses has been the inadequacy of current control strategies. In response to this problem, many advances have been made in developing complex signal processing algorithms to increase the amount of information that can be extracted from each channel of electromyographic (EMG) activity [1]–[3]. An alternative approach is to increase the number of independent EMG signals available to the controller. Preliminary studies on the use of nerve-muscle grafts as a possible method of achieving this are currently being conducted [4]. For this technique to work it is important that independent control signals can be obtained from each nerve-muscle graft and that crosstalk, the detection of volume conducted signals from muscles other than the muscle of interest, be kept to a minimum. The relative contributions of motor units (MUs) located throughout the muscle tissue to the surface EMG interference pattern, however, are not yet fully known. This issue is central in determining the feasibility of the proposed technique to successfully control multifunctional prostheses and is directly relevant to many other surface EMG applications.

One method of investigating the pick-up range of the surface EMG signal is to use model simulation. Anatomical properties and electrode configuration are both known to affect EMG crosstalk at the skin surface. The effect of interelectrode distance and increased selectivity of the surface EMG signal with double-differential or higher order spatial filters have been widely studied both experimentally and in model

Manuscript received July 15, 2002; revised December 15, 2002. This work was supported in part by the Whitaker Foundation under a Biomedical Engineering Research Grant, in part by the National Institute of Child and Human Development under Grant 1K08HD01224-01A1, and in part by the National Institute of Disability and Rehabilitation Research under Grant H133G990074-00. Asterisk indicates corresponding author.

*M. M. Lowery is with the Research Department, Rehabilitation Institute of Chicago, Chicago, IL 60611-4496 USA and also with the Department of Physical Medicine and Rehabilitation, Northwestern University, Evanston, IL 60201 USA (e-mail: m-lowery@northwestern.edu).

N. S. Stoykov is with the Research Department, Rehabilitation Institute of Chicago, Chicago, IL 60611-4496 USA and also with the Department of Physical Medicine and Rehabilitation, Northwestern University, Evanston, IL 60201 USA.

T. A. Kuiken is with the Rehabilitation Institute of Chicago, Chicago, IL 60611-4496 USA and also with the Departments of Physical Medicine and Rehabilitation and Electrical and Computer Engineering, Northwestern University, Evanston, IL 60201 USA.

Digital Object Identifier 10.1109/TBME.2003.812152

simulation [5]–[10]. The relationship between subcutaneous fat thickness and the electrode selectivity is less well established, although experimental studies have reported an increase in surface EMG selectivity with decreasing subcutaneous fat thickness [11], and increased crosstalk above muscles covered by large amounts of subcutaneous fat tissue [12].

In this paper, the pick-up volume of the surface EMG signal is explored to examine the feasibility of obtaining independent EMG signals from regions of muscle reinnervated by residual nerves following amputation. The model simulations serve as a means of exploring the detection volume of the surface EMG signal in a model where skin and fat tissue are included, and as a means of validating a new approach to EMG modeling, the finite-element method, against previously reported results based on analytical models.

II. METHODS

A. Single-Fiber Action Potentials (APs)

1) *Finite-Element Model*: Single-fiber APs were simulated using a finite-element model of the human upper arm comprised of concentric layers of bone, muscle, fat, and skin tissue [13]. A cylindrical bone of radius 10 mm was placed at the center of each model, surrounded by muscle tissue of radius 40 mm, subcutaneous fat and a layer of skin, 1.3 mm thick. The thickness of the subcutaneous fat layer was varied between 0 and 18 mm. Values for the conductivity of bone, muscle, fat, and skin were based on data reported by Gabriel *et al.* [14]. Muscle was assumed to be cylindrically anisotropic, with an anisotropy ratio of 5 and conductivity in the transverse direction of 0.25 S/m. Bone, fat, and skin were assumed to be isotropic, with conductivities of 0.02, 0.04, and 4.55×10^{-4} S/m, respectively [14]. The electric potential at each node in the model due to a propagating transmembrane current source was calculated using the finite-element method. The transmembrane current was described as a 150-point current source obtained by discretizing the analytical description of the second derivative of the transmembrane potential introduced by Rosenfalck [15]. The finite-element model was meshed and solved using the EMAS software package (Ansoft Corp., Pittsburgh, PA). Details of the finite-element model are provided in [13].

2) *Generation and Extinction of the AP*: The surface potential due to an AP propagating along a fiber of infinite length was calculated for each muscle fiber using the finite-element model. To fully describe the surface EMG signal, the generation and extinction of the AP at the fiber end-plate and tendon, respectively, should also be accounted for [16], [17]. The extracellular potential, $\phi(t)$, due to the propagating AP can be considered as the convolution of the transmembrane current, $i_m(t)$, and a weighting function, $w(t)$, which corresponds to the potential observed at the electrode due to a unit point source propagating along the muscle fiber [16], [18]

$$\phi(t) = \int_{-\infty}^{\infty} w(\tau) i_m(t - \tau) d\tau. \quad (1)$$

The weighting function for each muscle fiber, at each electrode location, was obtained by calculating the Fourier transform of the extracellular potential, $\Phi(j\omega)$, dividing by the Fourier transform of the transmembrane current, $I_m(j\omega)$, and taking the inverse Fourier transform (denoted \mathfrak{S}^{-1})

$$w(t) = \mathfrak{S}^{-1} \left(\frac{\Phi(j\omega)}{I_m(j\omega)} \right). \quad (2)$$

The propagating part of the AP waveform was recalculated as the sum of the convolution of the AP source and the weighting function between the fiber end-plate and each tendon, assuming propagation in

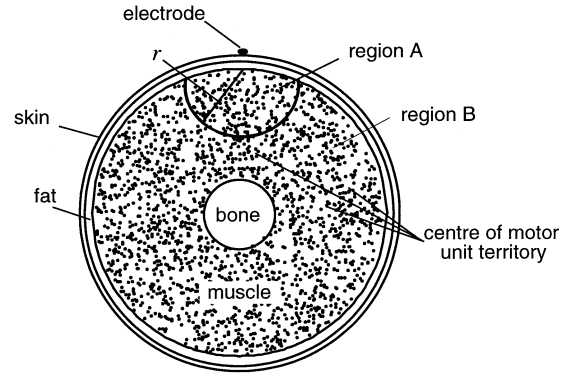


Fig. 1. Cross section through the model, normal to the fiber direction. Model geometry for 3-mm-thick layer of subcutaneous fat.

both directions away from the end-plate. The generation and extinction of the AP was accounted for by current compensation at the fiber end-plate and terminations using a similar approach to that described by Duchenne and Hogrel [19]. As each AP reached the end of the fiber, a source equal in magnitude and opposite in sign to the integral of the current along the fiber was multiplied by the weighting function at the fiber termination and added to the potential due to the propagating waveform. Similarly, as each AP began to propagate away from the fiber end-plate, a source equal in magnitude and opposite in sign to the integral of the current along the fiber was multiplied by the value of the weighting function at the fiber end-plate and added to the total extracellular potential.

B. Motor Unit Action Potentials (MUAPs)

It was assumed that all fibers in a MU were located at the same cross-sectional location and were of equal conduction velocity (4 m/s) and diameter (50 μm). The MUAP was obtained by summing together 500 single-fiber APs, located at the center of the MU territory. Fiber end-plates and terminations were randomly distributed throughout bands 5 mm wide located at the center and ends of the muscle fiber length, respectively, introducing a temporal dispersion of the single-fiber APs within each MUAP. All fibers were assumed to run the length of the muscle, which was chosen to be 300 mm, based on data for the biceps brachii. Extracellular potentials were calculated for fibers located at 15 depths, between 1 and 27.5 mm, below the surface of the muscle. The surface EMG signal was calculated at increments of 2.5° from the vertical axis. Using the symmetry of the volume conductor model, this yielded a series of MUAPs representing surface potentials generated by MUs located at each depth, at multiples of 2.5° from the vertical axis. A database of MUAPs was simulated in this manner for subcutaneous fat layers 0, 3, 9, and 18 mm thick.

C. Surface EMG Signal

To simulate voluntary surface EMG activity, 2000 identical MUs were randomly located throughout the muscle tissue, Fig. 1. The center of each MU was assumed to lie at the location of the closest simulated MU. MUs were assumed to be unsynchronized and to fire independently of one another. Mean MU firing rates were distributed linearly between 26 and 30 Hz and randomly assigned to each MU. The times between consecutive firings of a MU (interpulse intervals) were assumed to have a Gaussian distribution about the mean, based on the experimental observations of Clamann [20]. Voluntary EMG signals were simulated by firing each MU repetitively and summing together the signals from all MUs detected at each electrode. Data were generated for bipolar electrodes, oriented along the fiber direction, separated

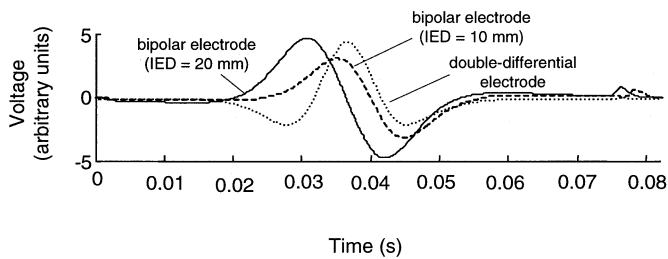


Fig. 2. Simulated surface APs for a muscle fiber located 10 mm below the surface of the muscle with a 3-mm-thick subcutaneous fat layer. Surface potentials are presented for bipolar electrodes 20 mm (solid line) and 10 mm (dashed line) apart, and for a double-differential electrode arrangement with an interelectrode distance of 10 mm (dotted line).

by interelectrode distances of 5, 10, and 20 mm, and for double-differential electrodes with an interelectrode distance of 10 mm. In each case, the distal electrode was located 80 mm from the center of the muscle end-plate region and 70 mm from the center of the end-plate zone. The root-mean-square (RMS), average rectified (AR), and mean-square value of the simulated data were calculated for epochs 1 s in duration.

III. RESULTS

An example of MUAPs simulated with different recording electrode configurations is illustrated in Fig. 2. To examine the electrode pick-up volume, the MUs were grouped into two muscles. Those lying within a volume of radius r , centered on the surface of the muscle directly below the electrodes were assumed to belong to the muscle of interest, denoted region A in Fig. 1. Those lying outside this area belonged to region B. The pick-up volume has been defined to facilitate reducing the region of active muscle in a consistent manner across all models. It should be noted, however, that the pick-up volume of the surface electrode in an inhomogeneous model is not cylindrical [21], but varies with the properties of the volume conductor.

A. Surface Electrode Pick-Up Volume

The radius of A, r , was varied until the RMS value of the surface EMG signal from region A was equal to 95% of the RMS value when all MUs in both regions A and B were active. Results are presented in Fig. 3 for subcutaneous fat layers 0, 3, 9, and 18 mm thick, using bipolar and double-differential electrode configurations. The means and standard deviations of eight sets of data, simulated for different random MU locations, are presented. The volume of muscle dominating the surface EMG signal increased as subcutaneous fat thickness was increased. Reducing the interelectrode distance yielded more focal recordings. In all models, the double-differential electrode arrangement was more selective than bipolar electrodes with an interelectrode distance of 10 or 20 mm, and more selective than the 5-mm interelectrode distance bipolar electrode with 9- and 18-mm-thick fat layers, Fig. 3.

B. Minimum Muscle Size for Independent Myoelectric Control Signals

In the control of myoelectric prostheses, EMG crosstalk and noise are commonly minimized by setting an activation threshold, above which the device is activated. This threshold is sufficiently high that the device is not accidentally activated, yet low enough that the user is not required to exert undue effort. To estimate a minimum volume of muscle from which independent EMG signals could be recorded, an activation threshold was defined as 5% of the surface EMG activity during maximal voluntary contraction (MVC) of the muscle of interest. By varying the value of the muscle radius, r , the

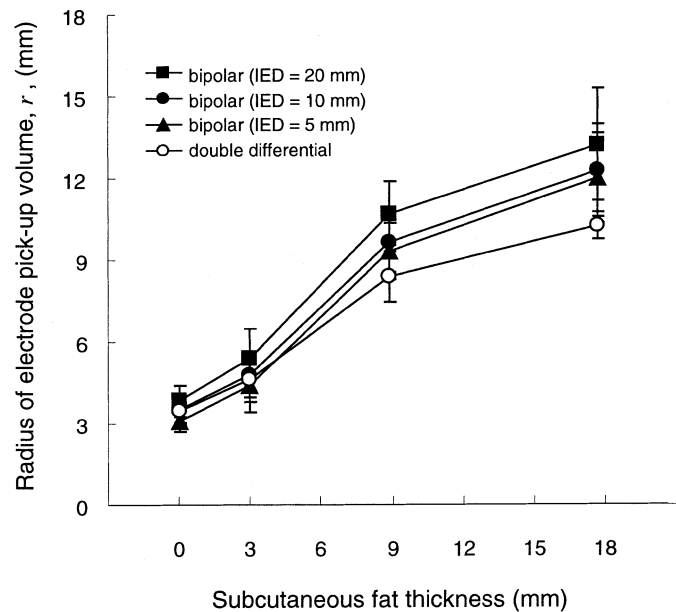


Fig. 3. Radius of region A for which the RMS value of the surface EMG signal from region A is equal to 95% of the EMG RMS amplitude when both region A and region B are active. Values are presented for different electrode configurations and for different values of subcutaneous fat thickness. The mean and standard deviations of eight sets of simulated data are presented.

size of the muscle for which the EMG activity during activation of all surrounding muscles was equal to 5% of the EMG activity during MVC of that muscle alone, was determined. Results were compared as EMG activity was quantified using the RMS, AR, and mean-square value of the signal, for different electrode configurations and subcutaneous fat thicknesses, Fig. 4. The minimum radius for which this condition was satisfied decreased as the thickness of the subcutaneous fat tissue was reduced, as the interelectrode distance was reduced and with a double-differential configuration. The smallest radii for which the EMG signal from the surrounding muscles fell below the 5% threshold level were observed when the mean square value, rather than the RMS or AR values, was employed, Fig. 4. The coefficients of variation of the AR, RMS, and mean square values calculated from 200 epochs of data generated using a single set of model parameters were 0.035, 0.036, and 0.072, respectively, for the 0- and 3-mm-thick fat layers; 0.045, 0.042, and 0.085 for the 9-mm-thick fat layer; and 0.059, 0.057, and 0.11 for the 18-mm-thick fat layer.

IV. DISCUSSION

Finite element analysis is a new approach to myoelectric signal modeling that has particular strengths in simulating complicated geometries, along with tissues with complex and inhomogeneous material properties. An analytical model of the surface EMG signal in a cylindrical two layer volume conductor was introduced by Gootzen *et al.* [17], and later extended to three layers [22], [23]. Fat and skin layers have also been included in a recent hemi-space model for planar geometries [24]. Although the relatively simple geometry of the generalized cylindrical limb may be modeled using analytical methods, the finite-element model remains numerically stable with the addition of a fourth structure, representing bone, and simultaneously calculates the electrical potential and current density at all nodes within the finite-element mesh. Previous simulations indicate that the influence of a bone located at the center of the volume conductor is slight, however, when located closer to the source and the skin surface the distribution of the surface EMG signal can be significantly altered [13]. Before extending

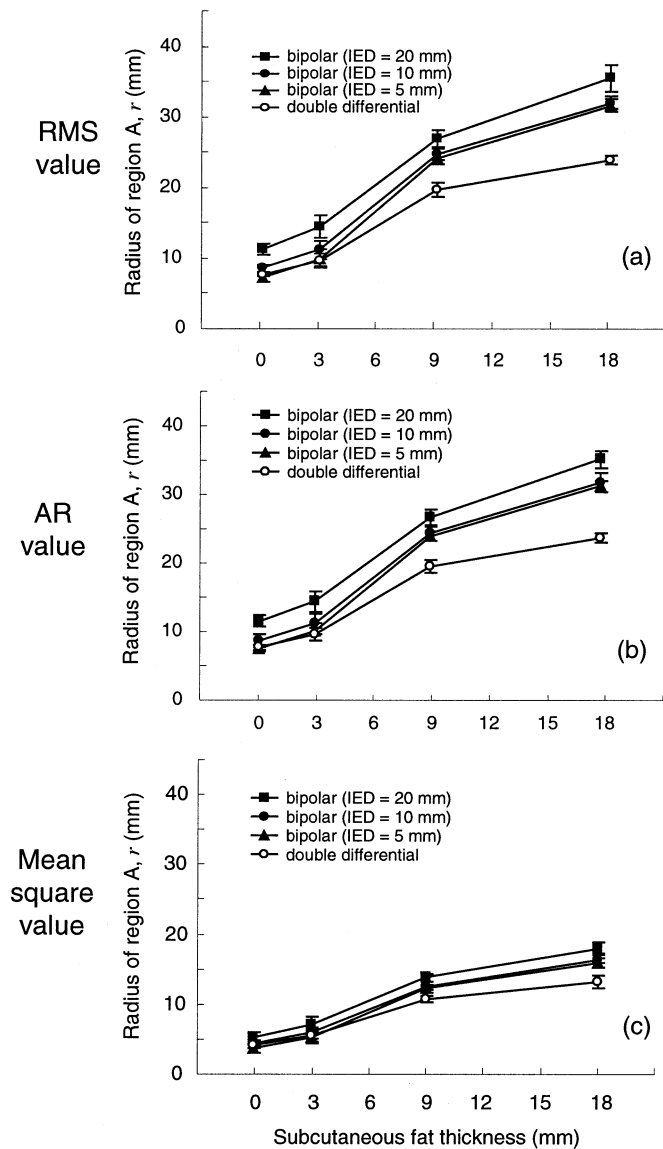


Fig. 4. Radius, r , for which (a) the RMS value (b) the AR value, and (c) the mean square value of the surface EMG signal from the surrounding muscles is equal to 5% of the EMG activity from that muscle alone. Values are presented for different electrode configurations as subcutaneous fat thickness is varied. The means and standard deviations of eight sets of simulated data are presented.

this approach to consider more complex models, it is important to confirm that the results are consistent with existing, well-established analytical models. To this end, the effect of electrode configuration, subcutaneous fat thickness and myoelectric control parameter on the pick-up range of the surface EMG signal has been explored to examine the feasibility of obtaining independent surface EMG signals from regions of reinnervated muscle for myoelectric control.

Interelectrode distance is known to alter the rate of decay of the surface EMG signal with increasing MU depth [8], [9]. Simulations were, therefore, conducted for different electrode configurations to investigate the combined interaction of interelectrode distance and subcutaneous fat thickness. The pick-up volume of the simulated surface EMG signal increased with increasing subcutaneous fat thickness, Fig. 3 and 4. As the distance between the electrode and muscle increases due to the presence of a thick layer of fat, there is a reduction in the relative differences in the distances between the electrode and fibers at different depths. The relative contribution of the most superficial MUs is, therefore, substantially reduced and the contribution of deeper MUs

increased. The increase in pick-up volume with subcutaneous fat thickness has important implications for EMG applications in general. EMG signals detected above regions covered by large amounts of fat tissue will be more susceptible to crosstalk from surrounding muscles, which is in agreement with experimental findings previously reported [11], [12]. Furthermore, EMG signals recorded above muscles where there is an association between fiber type and location may reflect different subpopulations of the MU pool if the variation in subcutaneous fat thickness among subjects is a large. An increased lateral spread of the potential from a single muscle fiber along the skin surface with increasing fat thickness was illustrated by Farina and Merletti [24]. This has similar implications for the effect of fat thickness on EMG selectivity, although in an inhomogeneous volume conductor the rate of decay of the surface potential with increasing source depth, examined here, and the rate of decay with increasing electrode displacement for a given source depth will be different.

The results confirm that the selectivity of surface EMG electrodes can be increased by reducing the interelectrode distance or by using a double-differential recording configuration. It is also clear that the effect of the electrode configuration depends on the thickness of subcutaneous fat tissue, Fig. 3 and 4. The effect of interelectrode distance on the surface EMG selectivity is consistent with results for single-fiber APs in an infinite volume conductor [5], [8]. Finally, the selectivity of the EMG signal depends on the observed EMG variable. The RMS and AR values yielded similar results, Fig. 4, as both are linearly related to the standard deviation of the EMG signal when the number of detected MUs is large. The radius for which the EMG signal from surrounding muscles was less than the 5% threshold value was substantially lower for the mean square value of the EMG signal, Fig. 4. This suggests that for the control paradigm considered here independent signals may be obtained from smaller muscles if the mean square value of the EMG signal is utilized, rather than the RMS or AR values of the EMG signal. It should be noted, however, that fluctuations in the output signal about the mean are higher if a square rather than square-root detector is employed, as indicated by an increase in the coefficient of variation by approximately a factor of two. Furthermore, while the contribution of each MU to the mean square value of the EMG signal may be established, as the mean square values sum linearly under independent MU activation, the relative contribution of each unit to the RMS value is not easily determined.

The EMG model has been simplified in many respects. To further refine the model, information about the size, fiber diameter, conduction velocity, and location of each active MU is required. Variations in some or all of these parameters may alter the results. Such detailed information, however, is not easily obtained. In its absence, the simplified model consisting of standardized MUs presented here yields a qualitative estimate of the pick-up volume of the different electrode configurations and of the approximate muscle size necessary for recording independent surface EMG signals in the upper arm. Considerable uncertainty surrounds the most suitable choice of material properties for the skin tissue in particular. Recent studies have reported skin conductivity substantially lower than that of muscle [14], [25]. However, in a comparison of simulated and experimentally recorded surface MUAPs, Roeleveld *et al.*, [22] observed that the experimental EMG signals decayed more slowly than simulated signals, unless a relatively high skin conductivity was used. A further consideration is the surface area of the recording electrodes, which have been modeled as point electrodes. Previous studies have shown little difference in electrode pick-up depth with increased electrode size [5], [8]. However, the shape of the pick-up volume will vary with electrode surface area, particularly for large recording surfaces.

The simulation results suggest that when there is little fat tissue between the electrode and the muscle, it should be possible to record

independent surface EMG control signals from superficial muscles lying within 5–10 mm of the surface of the muscle tissue, if selective electrode configurations and optimal EMG control parameters are employed. This is promising for the application of the nerve-muscle graft technique to the transhumeral amputee. Finally, while independence of the surface EMG signal is critical to this particular control paradigm, the role of crosstalk in more sophisticated control systems is more complex. In fact, volume conducted signals from neighboring muscles may provide additional information which can be utilized by multiple features and pattern-recognition-based class discrimination.

REFERENCES

- [1] B. Hudgins, P. Parker, and R. N. Scott, "A new strategy for multifunction myoelectric control," *IEEE Trans. Biomed. Eng.*, vol. 40, pp. 82–94, Jan. 1993.
- [2] K. Englehart, B. Hudgins, and P. A. Parker, "A wavelet-based continuous classification scheme for multifunction myoelectric control," *IEEE Trans. Biomed. Eng.*, vol. 48, pp. 302–311, Mar. 2001.
- [3] D. Graupe, J. Salah, and D. S. Zhang, "Stochastic analysis of myoelectric temporal signatures for multifunctional single-site activation of prostheses and orthoses," *J. Biomed. Eng.*, vol. 7, pp. 18–29, 1985.
- [4] T. A. Kuiken, N. S. Stoykov, M. Popovic, M. Lowery, and A. Taflove, "Finite element modeling of electromagnetic signal propagation in a phantom arm," *IEEE Trans. Neural Syst. Rehab. Eng.*, vol. 9, pp. 346–354, Dec. 2001.
- [5] P. A. Lynn, N. D. Bettles, A. D. Hughes, and S. W. Johnson, "Influences of electrode geometry on bipolar recordings of surface electromyogram," *Med. Biol. Eng. Comput.*, vol. 16, pp. 651–660, 1978.
- [6] H. Reucher, J. Silny, and G. Rau, "Spatial filtering of noninvasive multi-electrode EMG: part II—filter performance in theory and modeling," *IEEE Trans. Biomed. Eng.*, vol. BME-34, pp. 106–113, 1987.
- [7] C. J. De Luca and R. Merletti, "Surface myoelectric signal cross-talk among muscles of the leg," *Electroencephalogr. Clin. Neurophysiol.*, vol. 69, pp. 568–575, 1988.
- [8] A. J. Fuglevand, D. A. Winter, A. E. Patla, and D. Stashuk, "Detection of motor unit action-potentials with surface electrodes—influence of electrode size and spacing," *Biol. Cybern.*, vol. 67, pp. 143–153, 1992.
- [9] K. Roeleveld, D. F. Stegeman, H. M. Vingerhoets, and A. van Oosterom, "Motor unit potential contribution to surface electromyography," *Acta Physiol. Scand.*, vol. 160, pp. 175–183, 1997.
- [10] J. P. P. van Vugt and J. G. van Dijk, "A convenient method to reduce crosstalk in surface EMG," *Clin. Neurophysiol.*, vol. 112, pp. 583–592, 2001.
- [11] E. J. De la Barrera and T. E. Milner, "The effects of skinfold thickness on the selectivity of surface EMG," *Electroencephalogr. Clin. Neurophysiol.*, vol. 93, pp. 91–99, 1994.
- [12] M. Solomonow, R. Baratta, M. Bernardi, B. Zhou, Y. Lu, M. Zhu, and S. Acierno, "Surface and wire EMG crosstalk in neighboring muscles," *J. Electromyogr. Kinesiol.*, vol. 4, pp. 131–142, 1994.
- [13] M. M. Lowery, N. S. Stoykov, A. Taflove, and T. A. Kuiken, "A multiple-layer finite-element model of the surface EMG signal," *IEEE Trans. Biomed. Eng.*, vol. 49, pp. 446–454, May 2002.
- [14] S. Gabriel, R. W. Lau, and C. Gabriel, "The dielectric properties of biological tissues—Pt. 3: Parametric models for the dielectric spectrum of tissues," *Phys. Med. Biol.*, vol. 41, pp. 2271–2293, 1996.
- [15] P. Rosenfalck, "Intra- and extracellular potential fields of active nerve and muscle fibers. A physico-mathematical analysis of different models," *Acta Physiol. Scand.*, vol. Suppl 321, pp. 1–168, 1969.
- [16] G. V. Dimitrov and N. A. Dimitrova, "Precise and fast calculation of the motor unit potentials detected by a point and rectangular plate electrode," *Med. Eng. Phys.*, vol. 20, pp. 374–381, 1998.
- [17] T. Gootzen, D. F. Stegeman, and A. Vanoosterom, "Finite limb dimensions and finite muscle length in a model for the generation of electromyographic signals," *Electroencephalogr. Clin. Neurophysiol.*, vol. 81, pp. 152–162, 1991.
- [18] S. D. Nandedkar and E. Stalberg, "Simulation of single muscle-fiber action-potentials," *Med. Biol. Eng. Comput.*, vol. 21, pp. 158–165, 1983.
- [19] J. Duchene and J. Y. Hogrel, "A model of EMG generation," *IEEE Trans. Biomed. Eng.*, vol. 47, pp. 192–201, Feb. 2000.
- [20] H. P. Clamann, "Statistical analysis of motor unit firing patterns in a human skeletal muscle," *Biophys. J.*, vol. 9, pp. 1233–1251, 1969.
- [21] D. Farina, M. Fosci, and R. Merletti, "Motor unit recruitment strategies investigated by surface EMG variables," *J. Appl. Physiol.*, vol. 92, pp. 235–247, 2002.
- [22] K. Roeleveld, J. H. Blok, D. F. Stegeman, and A. van Oosterom, "Volume conduction models for surface EMG; confrontation with measurements," *J. Electromyogr. Kinesiol.*, vol. 7, pp. 221–232, 1997.
- [23] J. H. Blok, D. F. Stegeman, and A. van Oosterom, "Three-layer volume conductor model and software package for applications in surface electromyography," *Ann. Biomed. Eng.*, vol. 30, pp. 566–577, 2002.
- [24] D. Farina and R. Merletti, "A novel approach for precise simulation of the EMG signal detected by surface electrodes," *IEEE Trans Biomed Eng.*, vol. 48, pp. 637–646, June 2001.
- [25] V. Raicu, N. Kitagawa, and A. Irimajiri, "A quantitative approach to the dielectric properties of the skin," *Phys. Med. Biol.*, vol. 45, pp. L1–L4, 2000.